Simultaneous Detection of Anomaly Points and Fiber types in Multi-span Transmission Links Only by Receiver-side Digital Signal Processing

Takeo Sasai, Masanori Nakamura, Seiji Okamoto, Fukutaro Hamaoka, Shuto Yamamoto, Etsushi Yamazaki, Asuka Matsushita Hideki Nishizawa and Yoshiaki Kisaka
NTT Network Innovation Laboratories, NTT Corporation, 1-1 Hikari-no-oka, Yokosuka, Kanagawa, 239-0847 Japan
takeo.sasai.cp@hco.ntt.co.jp

Abstract: We experimentally demonstrate simultaneous localization of optical excess loss points and spans with different dispersion in multi-span fiber links using a neural-network based digital backpropagation. © 2020 The Author(s)

1. Introduction

As the application area of optical fiber transmission expands to data center interconnects and the capacity of the transmission system increases, simple and sophisticated transmission link analysis techniques are required [1, 2]. For example, if a transceiver can measure the loss profile along propagation direction of the fiber link, which used to be measured by a dedicated equipment such as optical time domain reflectometer (OTDR), it saves the equipment cost and human resources. In addition, monitoring during system operation could allow failure prediction in advance [3]. Accordingly, a power profile measurement method using only incoming signal to a receiver has been proposed and demonstrated [4]. As another example, the chromatic dispersion profile along the fiber propagation direction affects the maximum transmission distance and capacity. For example, in a link consisting of mixing of different fiber types of dispersion shifted fiber (DSF), non-zero (NZ) DSF, standard single mode fiber (SSMF), the fiber launch power is designed assuming the worst case profile to avoid fatal nonlinear distortion during fiber transmission. As a consequence, the transmission distance and the capacity used to be limited. If the chromatic dispersion profile along the propagation direction can be measured, the fiber launch power is optimized, and the distance and capacity can be maximized.

In this paper, we experimentally demonstrate the detection of not only lossy points but also dispersion shifted spans in the transmission lines when spans with different dispersions coexist. The experiment was conducted using dual polarization (DP) probabilistic shaping (PS) 64QAM 64-GBd with the net rate of 423.04 Gbps over 4-spans transmission links. The tested links are SSMF-only, DSF-inserted, and NZDSF-inserted links. The position of the non-SSMF spans is also switched. To emulate anomaly losses, 2-dB and 5-dB attenuators are inserted into each span. The detection can be achieved without any testing probes or measurement instruments, i.e., only by analysis of received signals.

2. Principle

Figure 1 (a) shows a schematic diagram of a neural-network-based digital backpropagation (NN-based DBP) [5]. In [5], weights of dispersion compensation filter in DBP is learned in the context of nonlinearity compensation but we focus on the learning of nonlinear coefficients γ_k and dispersion coefficients β_{2k}, where k = 1, 2,…N is the step number of the DBP. First, the input signal is propagated through standard DBP, setting γ_k to arbitrary initial values and β_{2k} to averaged values of estimated total dispersion (i.e., estimated total dispersion divided by the total number

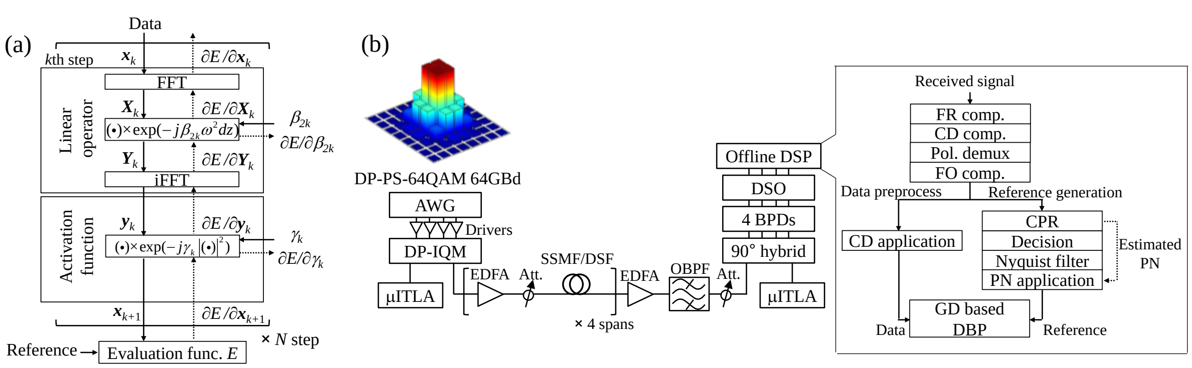

Fig. 1 (a) Block diagram of a neural-network-based DBP. (b) Experimental setup and block diagram of receiver side offline DSP.

of steps N). The mean square error (MSE) is then calculated for the evaluation function using the back-propagated signal and the reference waveform. How to get the reference waveform is explained in the next section. γ_k and β_{2k} are updated using gradient descent method as $\gamma_k(l+1) = \gamma_k(l) - \mu\, \partial E/\partial\gamma_k$, $\beta_{2k}(l+1) = \beta_{2k}(l) - \mu\, \partial E/\partial\beta_{2k}$, where l is the updating count, μ is the step size, and E is the evaluation function, i.e., the MSE. The partial differentiation $\partial E/\partial\gamma_k$ and $\partial E/\partial\beta_{2k}$ are calculated from differentiation of the output with respect to the input in each block using the chain rule [5]. This optimization scheme is simultaneous optimization of all γ_k and β_{2k} coefficients and offers rapid measurement compared to one-by-one optimization. From learned γ_k and β_{2k}, we can tell nonlinear phase rotation (NLPR) at each point and the spans with different dispersion in transmission lines. By subtracting the NLPR distribution with an unexpected loss in the transmission line from that for normal state, we can achieve "anomaly indicator" [4].

3. Experimental setup

Figure 1 (b) shows the experimental setup and block diagram of offline Rx-DSP. A PS-64-QAM 64-GBd signal was generated with the information rate of 3.305 bits and the entropy of 4.347 bits assuming a 21% FEC overhead [6]. Nyquist-pulse shaping was applied to the signal using a root-raised-cosine filter with a roll-off factor of 0.2. The frequency response of the transmitter was compensated right before emissions from a 120-GSa/s 4-ch arbitrary waveform generator (AWG) [7]. The generated electrical signal was boosted by 65-GHz differential driver amplifiers. Continuous waves from a micro-integrable tunable laser assembly (μITLA) with a 40-kHz linewidth were modulated by the signals with a DP-IQ modulator (IQM). The carrier wavelength was set to 1555.752 nm. The fiber input power was set to +5 dBm. The optical signal was launched into a straight transmission line consisting of SSMF (α = 0.199 dB/km, D = 16.90 ps/nm/km), DSF (α = 0.230 dB/km, D = 0.378 ps/nm/km), and NZDSF (α = 0.225 dB/km, D = 2.59 ps/nm/km). The details of the transmission lines are shown in Fig. 2 and Fig. 3.

At the receiver side, the signals were filtered by a 5-nm optical bandpass filter after post-amplification by an erbium doped fiber amplifier (EDFA) and converted into electrical signals via a coherent receiver composed of a 90° hybrid and 100-GHz-bandwidth balanced photo detectors (BPDs). The received signals were digitized by a 160-GSa/s digital sampling oscilloscope (DSO) and demodulated offline in Rx-DSP. The Rx frequency response (FR) compensation, chromatic dispersion (CD) compensation, adaptive equalization for linear equalization and for polarization de-multiplexing, and frequency offset (FO) compensation were performed. For learning coefficients of DBP, the signal was divided into two paths. One was the signal preprocess that restores the dispersion in the transmission line. The other was the reference signal generation for the NN-based DBP, which is composed of a standard demodulation process and regeneration of the transmitted signal waveform. The phase noise (PN) was again applied to the generated reference waveform using the estimated PN in carrier phase recovery (CPR). The preprocessed signal and the reference waveform were then fed into the NN-based DBP. μ and the length per step of DBP (distance resolution) were set to 1.0×10^{-3} and 2 km, respectively. A moving average was performed to the output of the DBP with a 5-step window size.

4. Results and Discussion

First, we obtained the NLPR distribution of a SSMF-only line with 70 km × 4 spans, as shown in Fig. 2 (a). The optical time domain reflectometer (OTDR) power profile was also provided for reference. In cases without any loss insertion (black solid line), the NLPR reflected amplification by EDFAs and attenuation of fibers. To investigate the capability of the lossy point detection, we inserted the 2-dB (green) and 5-dB (blue) attenuator at 50, 90, 190, and

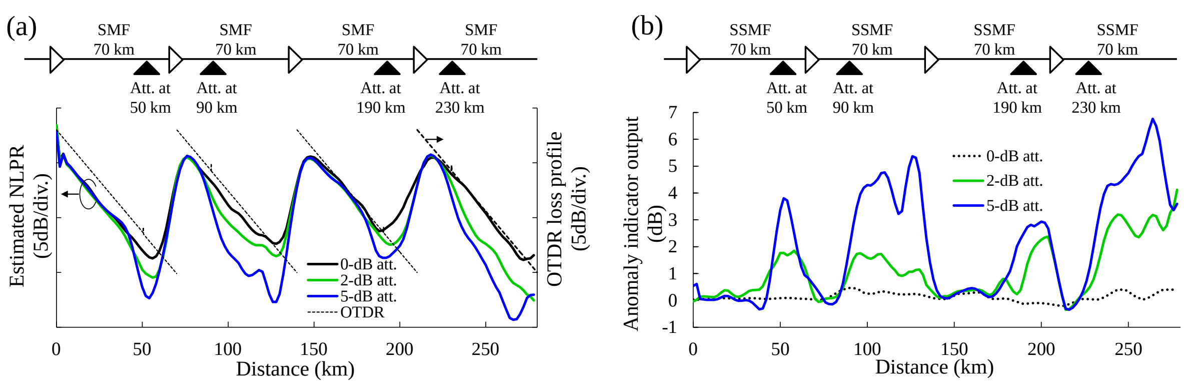

Fig. 2 (a) Estimated power profile and OTDR loss profile for reference and (b) deviation from normal state (0 dB attenuation) in 70 km × 4 spans transmission lines.

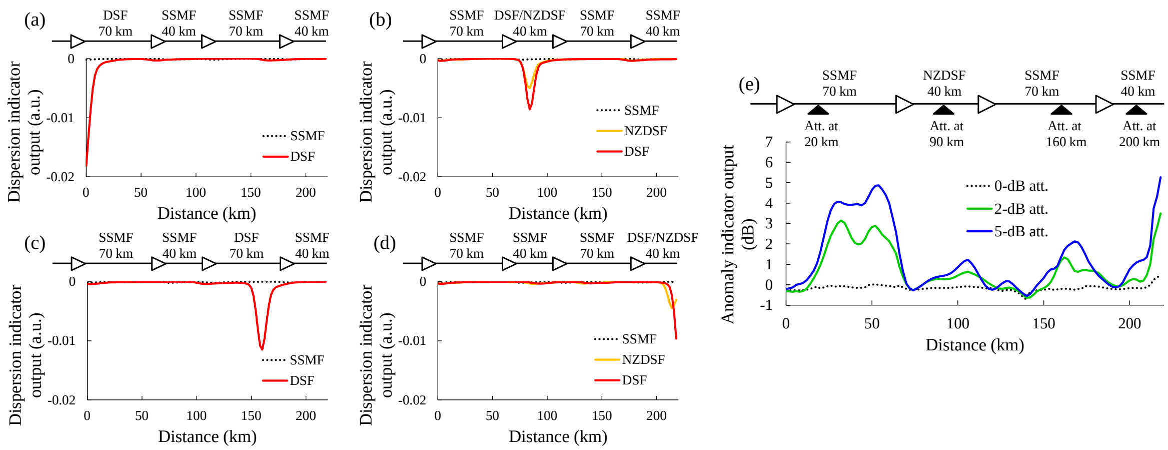

Fig. 3 Detection of DSF and NZDSF spans located in (a) first, (b) second, (c) third, and (d) fourth span in 4 spans of 220-km line. (e) Anomaly points detection in the transmission link with 40-km NZDSF in second span.

230 km. We can observe the NLPR reduction at loss points as optical power in the line decreases for abnormal cases. Figure 2 (b) shows the output of the anomaly indicator, i.e., the difference between the normal (0 dB attenuation) and abnormal conditions. Note that the beginning of the peak corresponds to the anomaly loss points. Successful localization of lossy points and detection of relative attenuation level were observed. The power profile fluctuated in the latter half of the second and fourth span. This is because nonlinearity was too small in the latter half of the spans due to accumulated attenuation by the fiber and attenuators, and this led to reduced measurement sensitivity.

Second, we investigated the capability of detecting DSF and NZDSF spans, as shown in Fig. 3 (a)-(d). The black-dashed line corresponds to the case with SSMF-only line, and the colored solid lines are the cases with the DSF (red) and NZDSF (yellow) coexisted in the transmission lines. The maximum value was normalized to zero. Compared to SSMF-only cases, the case where DSF and NZDSF coexisted clearly shows a sharp peak, which means there is lower dispersion fibers in the spans. When the dispersion shifted spans were located in the first or last spans of the link, the peak maximum was observed at the end of the spans (i.e., at 0 and 220 km). This was presumably because the adjacent span did not exist and the local dispersion estimation was not affected by the adjacent span. The peaks of NZDSF were smaller than those of DSF, indicating NZDSF has higher dispersion. Figure 3 (e) shows the detection of loss points in the presence of NZDSF in the second span. The attenuation was inserted at 20, 90, 160, and 200 km. Even in the presence of a dispersion shifted span, lossy points were successfully detected. However, in the NZDSF span, the peak was relatively weak compared to those of the other spans. The lower dispersion in the span makes estimated nonlinearity averaged over spans due to consecutive nonlinearity, thereby leading to the reduced measurement sensitivity. Even so, the sensitivity can be enhanced by switching the measurement channel to one with a longer wavelength.

5. Conclusion

We experimentally demonstrated the simultaneous detection of anomaly loss points and dispersion shifted spans in multiple-span transmission lines based on a NN-based DBP without any testing probe into fibers or additional instruments for measurement. This enables rapid and efficient network operation and helps with managing the nonlinearity budget in designing transmission systems.

6. References

[1] Z. Dong *et al.*, "Optical performance monitoring: a review of current and future technologies," *J. Ligthtw. Technol*., 34(2), pp 525-543, (2016).
[2] D. C. Kilper *et al*., "Optical physical layer SDN: Enabling physical layer programmability through open control systems," in Proc. of OFC 2017, W1H.3, (2017)
[3] A. Hirano, "Autonomous network diagnosis with AI," in Proc. of OFC 2019, Tu2E.4, (2019).
[4] T. Tanimura *et al.*, "Experimental demonstration of a coherent receiver that visualizes longitudinal signal power profile over multiple spans out of its incoming signal," in Proc. of ECOC 2019, PD.3.4, (2019).
[5] C. Hager *et al*., "Nonlinear interference mitigation via deep neural networks," in Proc. of OFC 2018, W3A.4, (2018).
[6] M. Nakamura *et al*., "Spectrally efficient 800 Gbps/carrier WDM transmission at 100-GHz spacing using probabilistically shaped PDM-256QAM," in Proc. of ECOC 2018, We3G.5 (2018).
[7] A. Matsushita *et al.*, "High-spectral-efficiency 600-Gbps/carrier transmission using PDM-256QAM format," *J. Ligthtw. Technol*., 37(2), pp 470-476, (2019).